Journal of Catalysis 260 (2008) 150–156

Contents lists available at ScienceDirect

Journal of Catalysis

www.elsevier.com/locate/jcat

Ru–Ti intermetallic catalysts for the selective hydrogenation of crotonaldehyde

J. Ruiz-Martínez [a], Y. Fukui [b], T. Komatsu [b], A. Sepúlveda-Escribano [a,*]

[a] Laboratorio de Materiales Avanzados, Departamento de Química Inorgánica, Universidad de Alicante, Apartado 99, E-03080 Alicante, Spain
[b] Department of Chemistry, Tokyo Institute of Technology, Ookayama, Meguro-ku, Tokyo 152-8550, Japan

ARTICLE INFO

Article history:
Received 6 June 2008
Revised 16 September 2008
Accepted 19 September 2008
Available online 18 October 2008

Keywords:
Intermetallic compound
Ruthenium
Titania
Crotonaldehyde hydrogenation

ABSTRACT

Titanium-doped ruthenium catalysts were prepared, characterized, and studied in the vapor-phase selective hydrogenation of crotonaldehyde. The catalysts were prepared by co-impregnation and by the chemical vapor deposition (CVD) method. XPS results indicate that titanium was well dispersed on the support for the catalyst prepared by CVD. Ruthenium dispersion was diminished by titanium addition, and a strong interaction of ruthenium with titanium was deduced from CO adsorption microcalorimetry. Results obtained in the vapor-phase hydrogenation of crotonaldehyde showed that the monometallic Ru catalyst had no selectivity toward crotyl alcohol, whereas the RuTi catalyst prepared by the CVD method gave the highest selectivity.

1. Introduction

Interest is growing in the use of heterogeneous catalysts for the synthesis of fine chemicals. One challenging task in this field is the selective hydrogenation of molecules with several functional groups. The production of allylic alcohols by the preferential hydrogenation of the C=O group in α,β-unsaturated aldehydes is very important, because these alcohols are valuable intermediates in the production of perfumes, flavorings, and pharmaceuticals [1–3].

Conventional hydrogenation catalysts based on noble metals, such as Ru, Pt, and Rh, are very active for these reactions, but they are not able to control the intramolecular selectivity by favoring the hydrogenation of the C=O instead of the C=C bond, because the hydrogenation of the C=C bond is thermodynamically favored [4]. Therefore, research efforts in this field have focused mainly on improving the selectivity to the unsaturated alcohol. There are three main ways of improving the selectivity toward unsaturated alcohols of noble metal-based catalysts. One is the use of large metal particles [5,6], which is assigned to electronic and steric effects. Another is the use of such supports as CeO_2 [7–9], TiO_2 [10,11], ZnO [12], MgO [13], or SnO_2 [14], which can modify the catalytic properties of the dispersed metal or bimetallic system.

The addition of a second metal that is more electropositive than the active one also can be useful in increasing the selectivity toward unsaturated alcohols, because the difference in electronegativity between both metals can enable polarization of the carbonyl group [15], thus facilitating its hydrogenation. In addition, geometrical effects, like a change in the metal dispersion [16,17] and decoration of the active metal by the second metal via surface enrichment [18], have been observed in bimetallic systems. The second metal can be in ionic state, as well as partially oxidized or in alloy or an intermetallic compound form.

An intermetallic compound (IMC) is a compound formed by two or more elements with simple composition and definite crystal structure that in many cases differs from that of its component metals, whereas the solid solution or alloy has the same crystal structure as one of the component metals. This specific crystal structure of IMC can give it unique catalytic properties, as it has been reported for some IMCs like CoGe [19], Pt_3Ge [20], Ni_3Sn [21], and $TiPt_3$ [22].

The present work was undertaken to study the promoting effect of titanium on a silica-supported ruthenium catalyst in the vapor-phase hydrogenation of crotonaldehyde. The catalysts were prepared by two different methods, with titanium incorporated by impregnation and by chemical vapor deposition (CVD). In a previous study [23], RuTi intermetallic compounds were found in the catalyst prepared by CVD, whereas this phase was not obtained in the catalyst prepared by conventional impregnation. The presence of Ti in the RuTi intermetallic compound also can modify the catalytic behavior of ruthenium. It was tested for Fisher–Tropsch synthesis, giving a higher selectivity to C^{2+} hydrocarbons compared with the monometallic Ru and to the RuTi catalyst, where the intermetallic compound was not found.

---

* Corresponding author. Fax: +34 965 90 34 54.
E-mail address: asepul@ua.es (A. Sepúlveda-Escribano).

0021-9517/$ – see front matter
doi:10.1016/j.jcat.2008.09.024

2. Experimental

2.1. Catalyst preparation

The monometallic Ru/SiO_2 catalyst was prepared by a pore-filling impregnation method. An aqueous solution containing ruthenium nitrosyl nitrate, $Ru(NO)(NO_3)$ (N.E. Chemcat Corp.), was added to silica gel (Cariact G-6, Fuji Silysia). The amount of the ruthenium solution was calculated to fill the pore of silica gel and to achieve a ruthenium loading of 5.0 wt%. The mixture was sealed by a piece of plastic film overnight at room temperature and then dried in an oven at 348 K for 12 h. The catalyst was put into a quartz flow reactor, and hydrogen was fed with a flow rate of 60 $\text{ml}\,\text{min}^{-1}$. The material was heated at 873 K for 2 h to reduce the ruthenium. Then it was cooled to room temperature with flowing hydrogen and kept in a drying desiccator.

Ru–Ti/SiO_2 was prepared by a co-impregnation method. An aqueous solution containing ruthenium nitrosyl nitrate and ammonium hexafluorotitanate, $(NH_4)_2TiF_6$ (Wako Pure Chemicals, 95%), was added to the silica gel. The amount of ruthenium was the same as that in Ru/SiO_2 and that of titanium was adjusted to an atomic ratio of Ti/Ru = 2. The drying and reduction procedures after its impregnation were the same as those for Ru/SiO_2. The catalyst prepared in this way is labeled Ru–Ti/SiO_2(IMP).

Ru–Ti/SiO_2 also was prepared by a CVD method in a similar manner to the preparation of Ni–Sn [24] and Pd–Fe [25] IMCs on silica gel. In a two-stage reactor, Ru/SiO_2 (0.70 g) prepared with the reduction at 873 K was put into the lower stage, and titanocene dichloride, $Ti(C_5H_5)_2Cl_2$ (Aldrich Chem., 0.86 g), was put into the upper stage. After Ru/SiO_2 was reduced with flowing hydrogen at 673 K for 30 min, the lower-stage temperature was set at a specific temperature (CVD temperature, 573 K). The temperature of titanocene dichloride was raised to 543 K (VAP temperature) for 1.5 h in flowing hydrogen to supply the vapor of titanocene dichloride onto Ru/SiO_2. Ti would be deposited through the hydrogenolysis of titanocene dichloride catalyzed by Ru/SiO_2. After the upper stage was cooled to room temperature, the lower stage was heated at 873 K for 1 h in flowing hydrogen. It was cooled to room temperature in flowing helium, and the resultant Ru–Ti/SiO_2 was kept in the drying desiccator. At this VAP temperature, the Ti/Ru atomic ratio obtained was 2.2. The catalyst prepared in this way is labeled RuTi/SiO_2(CVD).

2.2. Catalyst characterization

The chemical composition of the catalysts was determined by ICP (Rigaku, JY38S). The catalysts were dissolved as follows. Two pieces of sodium hydroxide were added to an aqueous solution of sodium hypochlorite. The catalysts were added to the solution slowly under stirring. After 2 h of stirring at room temperature, ethanol was added, and the stirring was continued for 30 min. Then hydrochloric acid was added to the slurry and it was stirred at 343 K until the black precipitate was dissolved and the solution color turned red. Finally, a small amount of hydrofluoric acid was added to the solution once it was at room temperature.

XPS spectra were acquired with a VG-Microtech Multilab 3000 spectrometer equipped with a hemispherical electron analyzer and a MgK_α 300 W ($h\nu = 1253.6$ eV, 1 eV $= 1.6302 \times 10^{-19}$ J) 300 W X-ray source. The powder samples were pressed into small Inox cylinders and then mounted on a sample rod placed in a pretreatment chamber and reduced in H_2 for 1 h at 773 K before being transferred to the analysis chamber. Before recording of spectra, the sample was maintained in the analysis chamber until a residual pressure of 5×10^{-9} mbar was reached. The spectra were collected at a pass energy of 50 eV. The intensities were estimated by calculating the integral of each peak, after subtraction of the S-shaped background, and by fitting the experimental curve to a combination of Lorentzian (30%) and Gaussian (70%) lines. All binding energies (BEs) were referenced to the Si 2p line at 103.5 eV, which provided BE values with an accuracy of ±0.2 eV. The surface Ru/Si and Ru/Ti ratios were estimated from the integrated intensities, after correction for atomic sensitivity factors [26].

TEM images were obtained with a JEOL JEM-2010 microscope using an acceleration voltage of 200 kV. The catalyst was previously reduced *ex situ* under hydrogen flow (50 $\text{ml}\,\text{min}^{-1}$) at 773 K for 1 h. After reduction, the catalyst was placed on a copper grid using suspensions of the catalysts in ethanol.

Differential heats of CO adsorption were measured at 298 K in a Setaram BT2.15D heat-flux calorimeter, as described in detail elsewhere [27]. This calorimeter was connected to a high-vacuum (base pressure $<10^{-6}$ Torr) volumetric system using Baratron capacitance manometers for precision pressure measurement ($\pm 10^{-3}$ Torr). The maximum apparent leak rate of the volumetric system (including the calorimetric cells) was 10^{-5} $\text{Torr}\,\text{min}^{-1}$ in a system volume of approximately 70 cm^3 (i.e., 10^{-5} $\mu\text{mol}\,\text{min}^{-1}$). The procedure for microcalorimetric measurements used in this study was as follows. Each sample (around 0.1–0.4 g) was treated ex situ in ultra-pure hydrogen (99.999% with further purification, AGA) for 1 h (5 $\text{K}\,\text{min}^{-1}$ ramp, 100 $\text{ml}\,\text{min}^{-1}$) at the desired temperature (773 K), after which the sample was purged for 1 h at the same temperature in ultra-high-purity helium (99.999% with further purification, AGA) to remove adsorbed hydrogen. Then it was sealed in a Pyrex NMR tube capsule and broken in a special calorimetric cell [27] once the sample had attained thermal equilibrium with the calorimeter. After the capsule was broken, the microcalorimetric data were collected by sequentially introducing small doses (1–10 μmol) of CO (99.5% with further purification, AGA) onto the sample until it became saturated. The resulting heat response for each dose was recorded as a function of time and integrated to determine the energy released (mJ). The amount of gas adsorbed (μmol) was determined volumetrically from the dose, equilibrium pressures, and system volumes and temperatures. The time required for the pressure to equilibrate in the calorimeter after each dose was approximately 1–15 min, and the heat response was monitored for 20–30 min after each dose to ensure that all heat was detected and to allow the heat response to return to the baseline value. The differential heat ($\text{kJ}\,\text{mol}^{-1}$), defined as the negative of the enthalpy change of adsorption per mole of gas adsorbed, was then calculated for each dose by dividing the heat released by the amount adsorbed.

The vapor-phase hydrogenation of crotonaldehyde (2-butenal) was tested in a microreactor at atmospheric pressure and operating under differential conditions. The catalyst (≈0.01 g) was reduced *in situ* at 773 K under flowing H_2 (50 $\text{ml}\,\text{min}^{-1}$) for 1 h and then cooled under H_2 to the reaction temperature (333 and 353 K). The hydrogenation reaction was carried out using a reaction mixture (total flow: 50 $\text{ml}\,\text{min}^{-1}$; H_2/aldehyde ratio of 26) of H_2 and crotonaldehyde (Fluka, >99.5%), which was prepared by passing H_2 through a thermostabilized saturator (293 K) containing crotonaldehyde. The concentration of reactants and products was determined by online gas chromatography with a Carbowax 20 M 58/90 semicapillary column.

3. Results and discussion

3.1. XPS results

Fig. 1 shows the XPS Ru 3d spectra of the monometallic Ru/SiO_2 catalyst, both unreduced and reduced, at 773 K. The spectra consist of the Ru $3d_{5/2}$ and Ru $3d_{3/2}$ bands appearing as a result of a spin-orbital splitting. The Ru $3d_{3/2}$ band is overlapped with the C 1s band at ∼284 eV derived from carbonaceous impurities (CH_x)

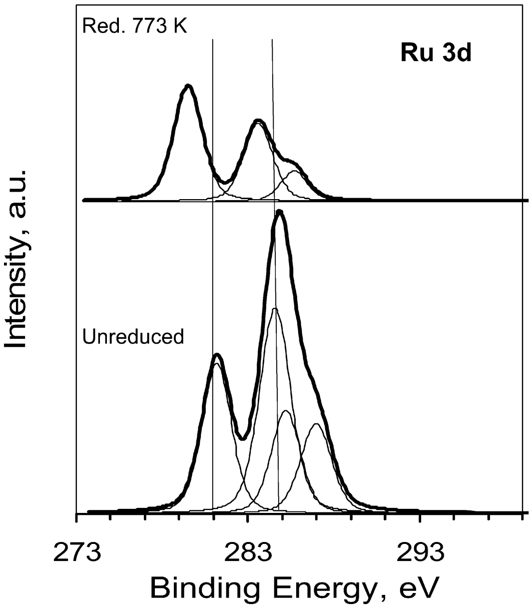

Fig. 1. XPS Ru 3d spectra for Ru/SiO_2 both unreduced and reduced at 773 K.

Table 1
XPS characterization.

Catalyst	Ru $3d_{5/2}$, eV	Ru/Si	Ti/Si	Ru/Ti
Ru/SiO_2				
Unreduced	281.2	0.012	–	–
Red. 773 K	279.5	0.020	–	–
$RuTi/SiO_2$(IMP)				
Red. 773 K	279.1	0.007	0.012	0.61
$RuTi/SiO_2$(CVD)				
Red. 773 K	280.3	0.011	0.029	0.38

originally present on the catalyst surface or slowly accumulated in the spectrometer. Consequently, only the values of Ru $3d_{5/2}$ band are used in the discussion that follows. In the case of the unreduced Ru/SiO_2 catalyst, a single band was detected at 281.2 eV that is assigned to oxidized Ru species (Ru(IV) or a lower oxidation state species). After reduction at 773 K for 1 h, the band was shifted to lower BEs (279.5 eV), with this contribution assigned to metallic ruthenium.

The ruthenium oxidation state for the titanium-doped catalysts also was studied after reduction at 773 K (Table 1). In both cases, the BEs correspond to ruthenium in metallic state. However, in the Ru–Ti/SiO_2(IMP) catalyst, the Ru $3d_{5/2}$ band is shifted to lower BEs than in the corresponding titanium-free counterpart. This shift could be a consequence of a larger ruthenium particle size compared with the titanium-free catalyst.

An opposite effect was found in the $RuTi/SiO_2$(CVD), in which the band was shifted to higher BEs. Although ruthenium is in the metallic state, this shift can be due to the formation of RuTi IMC.

The surface composition of the catalysts also was studied by XPS (Table 1). The surface Ru/Si atomic ratio can be considered a measure of the ruthenium dispersion on the silica gel support. This parameter decreases in the titanium-doped catalysts, thus indicating a loss of surface ruthenium with titanium addition. This effect can be explained by a partial coverage of the ruthenium particles by titanium species. On $RuTi/SiO_2$(CVD), this effect also can be explained by a diluting effect of the Ru due to the formation of a RuTi intermetallic compound. Komatsu et al. [23] found the formation of RuTi intermetallic compound when the catalyst was prepared by the CVD method. The decreased Ru/Si atomic ratio for the Ru–Ti/SiO_2(IMP) catalyst also can be ascribed to a larger ruthenium particle size. We discuss this effect in more detail in the presentation of TEM results.

The Ti/Si atomic ratio indicates the titanium dispersion on the silica gel support. It can be seen that the preparation method has a strong influence in the dispersion of titanium. The Ti/Si atomic ratio is 2.5 times higher in the catalyst prepared by CVD. The XPS results are in good agreement with XRD results reported in a previous work [23], where a half of titanium species in $RuTi/SiO_2$(CVD) were present as fine particles of RuTi IMC and the other half were present as oxidized titanium species too small to be detected by XRD, whereas Ru–Ti/SiO_2(IMP) gave XRD peaks of TiO_2 indicating the presence of large TiO_2 particles.

3.2. Transmission electron microscopy

Fig. 2 shows representative TEM micrographs of the catalyst reduced at 773 K in hydrogen for 1 h. The Ru/SiO_2 catalyst shows a highly uniform and wide dispersion of the metal particles. The particle size distribution of the metal in the supported catalyst was obtained by directly measuring the size of over 100 randomly chosen particles in the magnified TEM micrographs. The average diameter is 1.7 nm, and the particle size distribution is relatively narrow, as shown in Fig. 2. According to the histogram, 57% of Ru particles range in diameter from 1.4 to 2.0 nm. It can be concluded that this preparation method is suitable for dispersing ruthenium particles on silica gel.

For the Ru–Ti/SiO_2(CVD) catalyst, the average diameter of the metal particles is 2.1 nm. These particles also are homogeneously distributed on the surface of the support, but the particle size distribution is not as narrower as in the case of the monometallic catalyst. The increased particle size would be due to the possible creation of the intermetallic compound RuTi, as reported previously [23].

The catalyst prepared by the traditional co-impregnation method, Ru–Ti/SiO_2(IMP), shows a nonregular particle size and shape, and most of the nanoparticles observed are aggregated. The average diameter of the particles is 5.6 nm, much larger than in the other catalysts, which correlates with XPS results. The particle size distribution shows a wide size range (2–18 nm) of the ruthenium particles Thus, we conclude that this preparation method is not effective in obtaining well-dispersed ruthenium particles on this silica gel support.

TEM gives images of the metallic particles that allow calculation of their size. However, the number of metal surface sites cannot be evaluated from the metal particle sizes when titanium is present, because it can cover and/or dilute the ruthenium particles. A precise measurement of such a parameter can be obtained by CO chemisorption at room temperature.

3.3. CO chemisorption

Fig. 3 shows the CO chemisorption isotherms at 298 K for the catalysts reduced at 773 K for 1 h. It can be seen that the addition of titanium produces a decrease in the amount of CO chemisorbed, and this drop is more relevant in the catalyst prepared by co-impregnation. Ru dispersion (ratio between surface and total ruthenium atoms in the catalyst) can be assessed assuming a CO:Ru adsorption stoichiometry of 1:1 even though part of the CO was adsorbed as dicarbonyl species on Ru atoms in $RuTi/SiO_2$(CVD) [23].

It is interesting to observe that the relative amount of surface ruthenium decreased more than three times in the catalyst prepared by CVD compared with the monometallic one. Although a larger particle size was found in the bimetallic catalyst, it would be not consistent to consider the increase in particle size as the

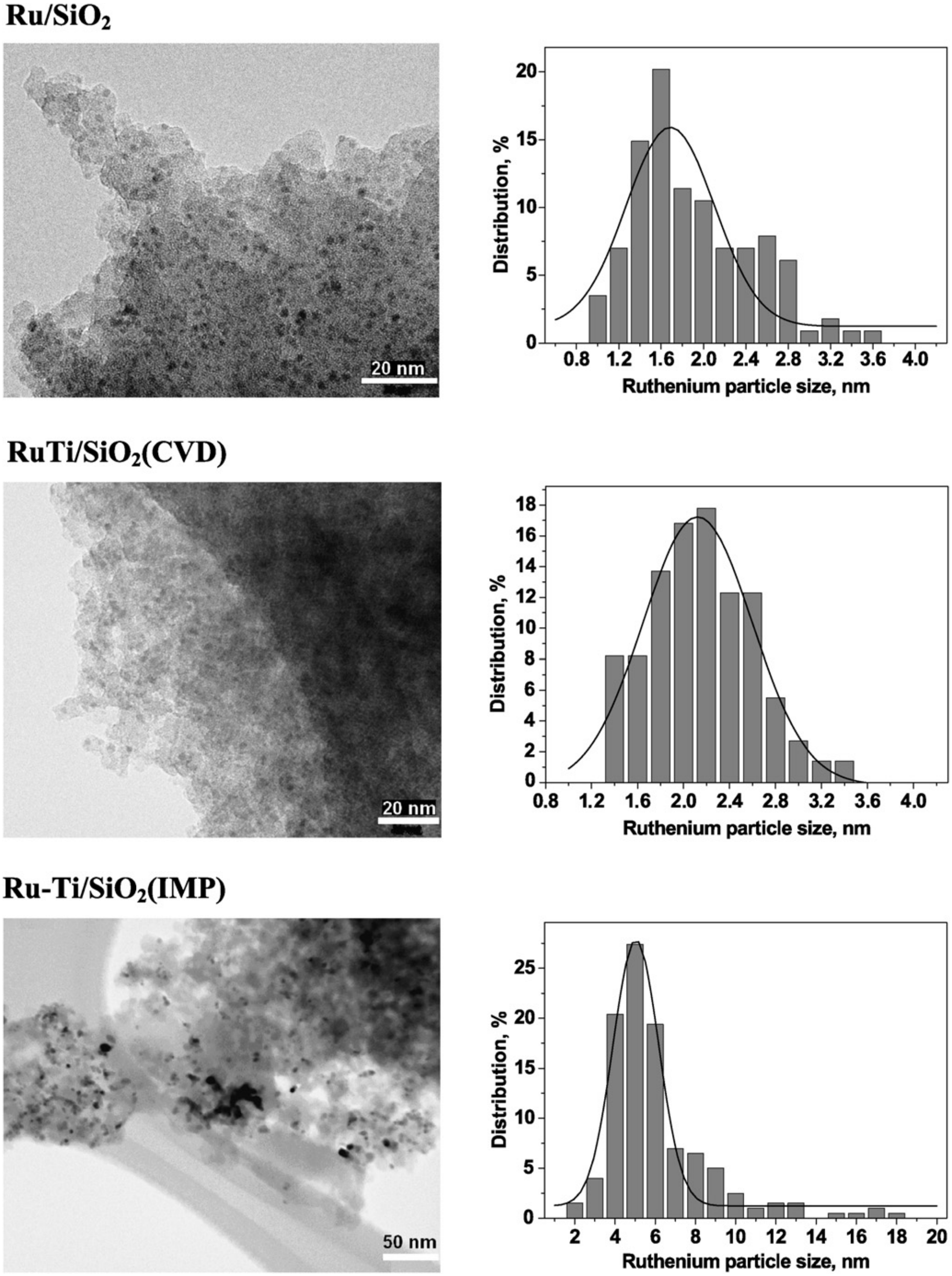

Fig. 2. TEM images and distribution of Ru particle sizes in the catalysts reduced at 773 K.

only effect involved in the lower ruthenium dispersion. A partial coverage of the ruthenium particle by titanium oxide species and the possible dilution of the ruthenium by the creation of a RuTi intermetallic compound also are suggested as the reasons for the decreased dispersion.

The existence of oxidized species of titanium close to the ruthenium particles, and even partially covering them, opens the possibility of a strong metal–support interaction effect that also would contribute to the decrease of the ruthenium dispersion. This effect would consist in the partial reduction of titanium dioxide in TiO_{2-x} species after reduction at high temperature (773 K). The interaction with the metal particles was explained on the basic of two different phenomena, (i) a charge transfer between the partially reduced support and the metal [28–30] and (ii) the coverage of the metal surface by patches of partially reduced support [31–33]. The literature reports this effect on titania-supported ruthenium catalysts [34–37], as well as in Ti-containing catalysts [38].

For the Ti-containing catalyst prepared by the co-impregnation method, the CO adsorption capacity is practically negligible compared with its counterparts, which reveals a very poor dispersion of the ruthenium in this catalyst. Because PtTi intermetallic compounds were not observed on previous studies [23], this result can be attributed to the presence of large ruthenium particles and also to the partial coverage of the ruthenium particles by titanium oxide species, as was discussed earlier for the other Ru–Ti catalyst.

3.4. CO adsorption microcalorimetry

To obtain information about the changes in the surface reactivity and energetic heterogeneity, CO adsorption microcalorimetry was performed at 298 K. Small doses of CO were introduced on

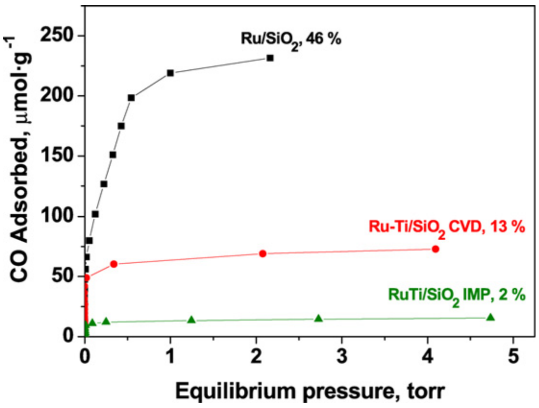

Fig. 3. CO chemisorption isotherms at 298 K for the catalysts reduced at 773 K; dispersion is also noted as percentage.

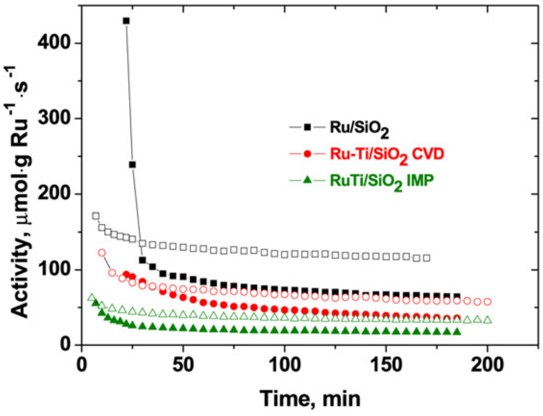

Fig. 5. Evolution of activity in crotonaldehyde hydrogenation with time on-stream at 333 (full symbols) and 353 K (open symbols) for the catalysts reduced at 773 K.

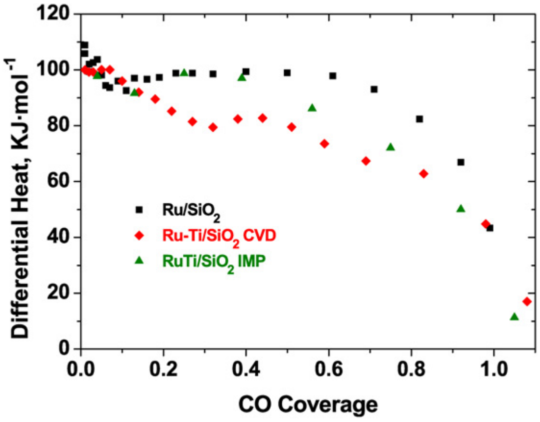

Fig. 4. Differential heats of CO adsorption as a function of the adsorbate coverage at 298 K for the catalysts reduced at 773 K.

the reduced catalyst and the differential heat of adsorption was measured as a function of the CO coverage. Due to the difference adsorption capacities of the catalysts, the heat of adsorption has been represented as a function of the monolayer coverage (Fig. 4). This procedure facilitates comparisons of catalysts with very different dispersions. The full coverage of the monolayer is considered when the heat of CO adsorbed reaches the value of physisorption (about 40 kJ/mol).

The heat of adsorption versus coverage profile for the monometallic Ru/SiO$_2$ catalyst shows the highest initial heat of adsorption ($\approx$110 kJ/mol) and dramatically decreases down to a plateau at around 100 kJ/mol. The constant value of the plateau is extended over a wide range of surface coverage (from 0.05 to 0.6), and then the heat of adsorption decreases until saturation is reached. The large extension of the plateau reveals a highly energetic homogeneity of the surface metal atoms, and the high initial heat of adsorption observed can be attributed to the interaction of CO with highly energetic sites, like metal atoms at corners and edges [39,40].

It is interesting to observe that the addition of titanium to the catalysts produces significant differences in the heat of adsorption profiles. The initial heats of adsorption are lower (around 100 kJ/mol) in both Ti-containing catalysts. This fact can be ascribed either to coverage or interaction of titanium species with highly energetic ruthenium atoms (geometric or electronic interaction). The microcalorimetric results for the RuTi/SiO$_2$(CVD) catalyst reveal two well-defined plateaus, one appearing at the same value than in the monometallic catalyst (100 kJ/mol) and the other appearing at 80 kJ/mol. These findings indicate a higher energetic heterogeneity of the surface metal atoms, as well as the creation of new low-energetic sites possibly due to a strong interaction between ruthenium and titanium that weakens the CO adsorption strength.

Microcalorimetric results for the adsorption of CO on RuTi/SiO$_2$-(IMP) catalyst show a plateau of nearly constant heat around 100 kJ/mol that extends up to coverage $\approx$0.4, after which the heat decreases to saturation. In this case, the heat of adsorption versus coverage profile is rather similar to that corresponding to the monometallic catalyst. However, the Ru/SiO$_2$ catalyst shows higher heat of adsorption over a coverage of 0.4. This result can be explained on the basis of a strong interaction between ruthenium and titanium atoms, although the presence of larger ruthenium particles, as described in the TEM section, also would account for this effect. Thus, a larger ruthenium particle size would increase the coordination number of the surface atoms, and it is well known that the heat of adsorption increases with decreasing the average coordination number of the surface metal atoms, due to preferential adsorption on low-coordination sites like edges and corners [41].

3.5. Crotonaldehyde hydrogenation

The catalytic behavior of the catalysts, after reduction at 773 K, in the selective hydrogenation of crotonaldehyde at 333 and 353 K is reported. In all cases, data have been obtained after the carbon balance was achieved. Before this, some proportions of reactant and products were adsorbed on the catalyst, and no reliable measurements could be performed.

Fig. 5 shows the evolution of the catalytic activity as a function of time on stream at different reaction temperatures. During the first period on stream (around 50 min), the catalysts deactivate, but subsequently, the reaction reached a quasi-steady state. This effect is especially significant for the monometallic Ru/SiO$_2$ catalyst, whose activity at 333 K decreased more than fourfold.

The highest activity is obtained for the monometallic catalyst, followed by RuTi/SiO$_2$(CVD) and Ru–Ti/SiO$_2$(IMP). These data are in agreement with the dispersion results. However, when the catalytic activity is analyzed in terms of turnover frequency (molecules of crotonaldehyde reacting per surface ruthenium atom per time), reported in Table 2, these numbers are higher in the case of the titanium-doped catalysts, which means that the addition of titanium has created new active sites, probably at the ruthenium–titanium interface, which are more active in the reaction. Note that the TOF decreases rapidly in the monometallic catalyst. The catalyst deactivation in this system has been related to the irreversible adsorption of organic molecules on the catalyst surface [5,42], and also to the decarbonylation of the reactant molecules yielding car-

Table 2
Turnover frequencies at different times on-stream.

Catalyst	Initial TOF-10^2 (s^{-1})	TOF-10^2 at 100 min (s^{-1})
Ru/SiO_2	9.4	1.6
RuTi/SiO_2(IMP)	25.4	8.7
RuTi/SiO_2(CVD)	10.2	3.5

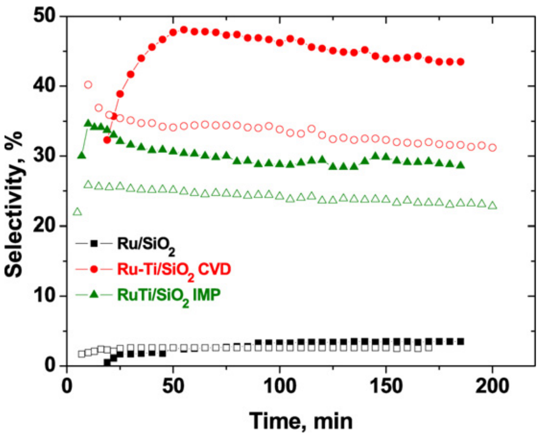

Fig. 6. Evolution of selectivity toward crotyl alcohol for crotonaldehyde hydrogenation with time on-stream at 333 (full symbols) and 353 K (open symbols) for the catalysts reduced at 773 K.

bon monoxide, which is irreversibly adsorbed under the reaction conditions, poisoning the active sites [5]. The results obtained by CO adsorption microcalorimetry demonstrate a stronger interaction of CO with the monometallic catalyst. This finding suggests that the strong deactivation would be due in some part to the presence of CO strongly adsorbed on the active sites.

The titanium addition and the preparation method not only affect the catalytic activity; the selectivity toward crotyl alcohol also is affected in great extension by these parameters. The hydrogenation of crotonaldehyde can yield a series of products. Thus, hydrogenation of the olefinic C=C bond yields butanal, whereas the hydrogenation of the carbonyl C=O bond yields crotyl alcohol. These compounds can be further hydrogenated to produce butanol. Moreover, decarbonylation and cracking also may take place, yielding light hydrocarbons (C_{1-3}). The extent of the secondary reactions depends on the total conversion, and thus the selectivity toward crotyl alcohol usually decreases as the conversion increases [4,43,44].

The products obtained by the reaction condition used in this study were butanal, crotyl alcohol, butanol, and a very small amount of light hydrocarbons C_{1-4}. The evolution of selectivity toward crotyl alcohol as a function of time on stream for the catalysts at 333 and 353 K is shown in Fig. 6. The monometallic catalyst shows practically no selectivity toward crotyl alcohol (around 3%). Butanol is produced at the first stages of the reaction, but sharply decreases (see Table 3) with the decrease in activity, and after 100 min on stream, only the olefinic C=C double bond is selectively hydrogenated, yielding butanal. This is the expected behavior for monometallic ruthenium catalysts in the absence of any support effect, and similar results have been reported on the literature. Bachiller-Baeza et al. [45] found no selectivity toward crotyl alcohol on ruthenium over graphite and activated carbon; the same results were reported by Riguetto et al. [46] with ruthenium on silica.

An enhanced selectivity toward crotyl alcohol is found in the titanium-containing catalysts. The Ru–Ti/SiO_2(IMP) catalyst has a selectivity toward crotyl alcohol of around 30%, which remains practically constant with time on stream. Kaspar et al. [47] studied the promoting effect of titanium in ruthenium catalysts for this kind of reaction and found an enhanced selectivity toward the unsaturated alcohol after reduction at high temperature. The authors suggested a decoration of metal particles by titania suboxides as the reason for this selectivity for the carbonyl group hydrogenation. A similar model also can be used to explain the observed behavior of the titanium-impregnated catalysts in this study; the presence of titania suboxides can interact with the C=O bond and thus enhance its hydrogenation.

The best selectivity toward crotyl alcohol was obtained for the RuTi/SiO_2(CVD) at 333 K. At the fist stages of the reaction, the selectivity was low; the high conversion promotes the rehydrogenation of crotyl alcohol into butanol. It increases with the time on stream until it reaches a maximum of around 48% and then decreases slightly thereafter. This increased selectivity compared with its titanium-impregnated counterpart can be explained by two factors: (i) better dispersion of titanium on silica surface and (ii) formation of RuTi intermetallic compounds. Bearing in mind the XPS results, better dispersion of titanium was seen for the catalyst prepared by the CVD method; this result also is supported by XRD studies reported previously [23]. This high dispersion increases the likelihood of an interaction between the ruthenium particles and titanium and thus an increase in the selectivity toward crotyl alcohol. This strong ruthenium–titanium interaction is also proved by adsorption microcalorimetry, where the heat of adsorption of CO was lower compared with that of the other catalysts over a wide range of coverage. The promoting effect of the formation of RuTi intermetallic compounds is not straightforward, and it is difficult to understand how it can influence the selectivity toward the hydrogenation of the carbonyl bond, because the factor discussed previously also affects this. Formation of RuTi intermetallic compound may help decrease the activity for the hydrogenation of the C=C bond, as has been shown in Ru–Sn [46] and Pt–Sn [48,49] systems. The dilution of ruthenium by titanium would decrease the amount of sites that are able to hydrogenate the C=C bond. These sites are unmodified or slightly modified ruthenium ensembles, and the formation of RuTi intermetallic compound would destroy them, slowing the rate of C=C hydrogenation. A similar retardation of C=C bond hydrogenation has been reported for IMCs of CoGe [19], Ni_3Sn, Ni_3Sn_2, and Ni_3Sn_4 [24] in the hydrogenation of acetylene and Pt_3Ge, Pt_2Ge, and PtGe [20] in the hydrogenation of 1,3-butadiene.

The effect of the reaction temperature in the activity and selectivity toward crotyl alcohol (Figs. 5 and 6) also has been studied. The increase in reaction temperature causes an increase in the catalytic activity and a decrease in the selectivity toward crotyl alcohol. The formation of butanal was favored over that of crotyl alcohol, due to the differing activation energies for the hydrogenation of the olefinic and carbonyl bonds (30.8 and 42.3 $kJ\,mol^{-1}$, respectively).

Finally, it is necessary to mention that the overall conversion was maintained during all catalytic tests in a range in which the selectivity was not affected by the conversion (from 2 to 10%).

4. Conclusion

This work reports the promoting effect of titanium on a ruthenium over silica gel catalyst in the vapor-phase hydrogenation of crotonaldehyde. The titanium-containing catalysts were prepared by traditional impregnation methods and by the CVD of titanium. XPS measurements revealed the presence of ruthenium in the metallic state after reduction at 773 K, along with a wider dispersion of titanium in the catalyst prepared by CVD. Ruthenium dispersion was diminished by titanium addition, possibly due to a partial covering of the ruthenium particles by titanium oxide species, as well as to the possible formation of RuTi intermetallic

Table 3
Selectivity and yield of crotyl alcohol at different times on-stream.

Catalyst	Selectivity (%)								CROTOL yield (%)	
	Initial				100 min				Initial	100 min
	HC	Butanal	Butanol	CROTOL	HC	Butanal	Butanol	CROTOL		
Ru/SiO_2	1	47	51	1	3	93	2	3	0.47	0.24
RuTi/SiO_2(IMP)	2	49	19	30	3	65	3	29	1.62	0.52
RuTi/SiO_2(CVD)	2	45	21	32	3	48	3	46	3.36	2.22

compounds. TEM also showed that a wider particle size distribution also was involved in this loss of ruthenium dispersion for the impregnated catalyst. CO adsorption microcalorimetry results suggest a stronger interaction of ruthenium with titanium for the catalyst prepared by the CVD method. The activity and selectivity toward crotyl alcohol in the selective hydrogenation of crotonaldehyde in the vapor phase also was altered by titanium addition. No selectivity for the monometallic catalyst was found; as long as the activity decreased with the addition of titanium, the selectivity increased. The effect of the preparation method was significant. The selectivity for the catalyst prepared by CVD was increased significantly. Two factors are suggested as being responsible for this improvement: (i) better dispersion of titanium on the silica surface and (ii) formation of RuTi intermetallic compounds.

Acknowledgments

Financial support from Ministerio de Educación y Ciencia (Project NAN2004-09267-CO3) and Generalidad Valenciana (Project ACOM2007/049), Spain, is gratefully acknowledged.

References

[1] S. Galvagno, G. Capannelli, G. Neri, A. Donato, R. Pietropaolo, J. Mol. Catal. 64 (1991) 237.
[2] P. Gallezot, D. Richard, Catal. Rev. Sci. Eng. 40 (1998) 81.
[3] P. Claus, Top. Catal. 5 (1998) 51.
[4] M.A. Vannice, B. Sen, J. Catal. 115 (1989) 65.
[5] M. Englisch, A. Jentys, J.A. Lercher, J. Catal. 166 (1997) 25.
[6] P. Claus, H. Hofmeister, J. Phys. Chem. B 103 (1999) 2766.
[7] A. Sepúlveda-Escribano, F. Coloma, F. Rodríguez-Reinoso, J. Catal. 178 (1998) 649.
[8] M. Abid, R. Touroude, Catal. Lett. 69 (2000) 139.
[9] J. Silvestre-Albero, F. Rodríguez-Reinoso, A. Sepúlveda-Escribano, J. Catal. 210 (2002) 127.
[10] A. Huidobro, A. Sepúlveda-Escribano, F. Rodríguez-Reinoso, J. Catal. 212 (2002) 94.
[11] A. Dandekar, M.A. Vannice, J. Catal. 183 (1999) 344.
[12] M. Consonni, D. Jokic, D.Y. Murzin, R. Touroude, J. Catal. 188 (1999) 165.
[13] N. Homs, J. Llorca, P. Ramírez de la Piscina, F. Rodríguez-Reinoso, A. Sepúlveda-Escribano, J. Silvestre-Albero, Phys. Chem. Chem. Phys. 3 (2001) 1782.
[14] K. Liberková, R. Touroude, J. Mol. Catal. A Chem. 180 (2002) 221.
[15] M.d.C. Aguirre, P. Reyes, M. Oportus, I. Melián-Cabrera, J.L.G. Fierro, Appl. Catal. A Gen. 233 (2002) 183.
[16] S. Recchia, C. Dossi, N. Poli, A. Fusi, L. Sordelli, R. Psaro, J. Catal. 184 (1999) 1.
[17] P. Reyes, G. Pecchi, J.L.G. Fierro, Langmuir 17 (2001) 522.
[18] P. Maki-Arvela, L.P. Tiainen, M. Lindblad, K. Demirkan, N. Kumar, R. Sjoholm, T. Ollonqvist, J. Vayrynen, T. Salmi, D.Y. Murzin, App. Catal. A 241 (2003) 271.
[19] T. Komatsu, Y. Fukui, T. Yashima, Stud. Surf. Sci. Catal. 101 (1996) 1095.
[20] T. Komatsu, S. Hyodo, T. Yashima, J. Phys. Chem. B 101 (1997) 5565.
[21] A. Onda, T. Komatsu, T. Yashima, J. Catal. 201 (2001) 13.
[22] T. Komatsu, D. Satoh, A. Onda, Chem. Commun. (2001) 1080.
[23] T. Komatsu, Y. Fukui, Appl. Catal. A 279 (2005) 173.
[24] A. Onda, T. Komatsu, T. Yashima, J. Catal. 221 (2004) 378.
[25] T. Komatsu, K. Inaba, T. Uezono, A. Onda, T. Yashima, Appl. Catal. A 251 (2003) 315.
[26] D. Briggs, M.P. Seah, Practical Surface Analysis, vol. 1, second ed., Wiley, 1993.
[27] B.E. Spiewak, J.A. Dumesic, Thermochim. Acta 290 (1996) 43.
[28] W. Jochum, D. Eder, G. Kaltenhauser, R. Kramer, Top. Catal. 46 (2007) 49.
[29] J.M. Herrmann, M. Gravell-Rumeau-Maillot, P.C. Gravelle, J. Catal. 104 (1987) 136.
[30] P. Chou, M.A. Vannice, J. Catal. 104 (1987) 1.
[31] A.J. Simoens, R.T.K. Baker, D.J. Dwyer, C.R.F. Lund, R.J. Madon, J. Catal. 86 (1984) 359.
[32] R. Green, P. Morrall, M. Bowker, Catal. Lett. 98 (2004) 129.
[33] J. Santos, J. Phillips, J.A. Dumesic, J. Catal. 81 (1983) 147.
[34] E. Kikuchi, M. Matsumoto, T. Takahashi, A. Machino, Y. Morita, Appl. Catal. 10 (1984) 251.
[35] G.C. Bond, R.R. Rajaram, R. Burch, J. Phys. Chem. 90 (1986) 4877.
[36] C.C.A. Riley, P. Jonsen, P. Meehan, J.C. Frost, K.J. Packer, Catal. Today 9 (1991) 121.
[37] D. Li, N. Ichikuni, S. Shimazu, T. Uematsu, Appl. Catal. A 180 (1999) 227.
[38] S.M. Gheno, S. Damyanova, B.A. Riguetto, C.M.P. Marques, C.A.P. Leite, J.M.C. Bueno, J. Mol. Catal. A Chem. 198 (2003) 263.
[39] A. Guerrero-Ruiz, A. Maroto-Valiente, M. Cerro-Alarcón, B. Bachiller-Baeza, I. Rodríguez-Ramos, Top. Catal. 19 (2002) 303.
[40] J.C. Serrano-Ruiz, G.W. Huber, M.A. Sánchez-Castillo, J.A. Dumesic, F. Rodríguez-Reinoso, A. Sepúlveda-Escribano, J. Catal. 241 (2006) 378.
[41] J.L. Gland, M.R. McClellan, F.R. McFeely, J. Vac. Sci. Technol. A 1 (1983) 1070.
[42] F. Coloma, J. Llorca, N. Homs, P. Ramírez de la Piscina, F. Rodríguez-Reinoso, A. Sepúlveda-Escribano, Phys. Chem. Chem. Phys. 2 (2000) 3063.
[43] F. Coloma, A. Sepúlveda-Escribano, J.L.G. Fierro, F. Rodríguez-Reinoso, Appl. Catal. A 136 (1996) 231.
[44] F. Coloma, A. Sepúlveda-Escribano, J.L.G. Fierro, F. Rodríguez-Reinoso, Appl. Catal. A 148 (1996) 63.
[45] B. Bachiller-Baeza, A. Guerrero-Ruiz, I. Rodríguez-Ramos, Appl. Catal. A 192 (2000) 289.
[46] B.A. Riguetto, C.E.C. Rodrigues, M.A. Morales, E. Baggio-Saitovitch, L. Gengembre, E. Payen, C.M.P. Marques, J.M.C. Bueno, Appl. Catal. A 318 (2007) 70.
[47] J. Kaspar, M. Graziani, J. Mol. Catal. 72 (1992) 243.
[48] J. Ruiz-Martínez, A. Sepúlveda-Escribano, J.A. Anderson, F. Rodríguez-Reinoso, Catal. Today 123 (2007) 235.
[49] J. Ruiz-Martínez, F. Coloma, A. Sepúlveda-Escribano, J.A. Anderson, F. Rodríguez-Reinoso, Catal. Today 133–135 (2008) 35.